NATIONAL ADVISORY COMMITTEE FOR AERONAUTICS

TECHNICAL MEMORANDUM

No. 1089

INVESTIGATION OF FLOW IN A CENTRIFUGAL PUMP

By Karl Fischer

Mitteilungen des Hydraulischen Instituts der
Technischen Hochschule, München
No. 4, 1931
Verlag von R. Oldenbourg, München und Berlin

Washington
July 1946

NATIONAL ADVISORY COMMITTEE FOR AERONAUTICS

TECHNICAL MEMORANDUM NO. 1089

INVESTIGATION OF FLOW IN A CENTRIFUGAL PUMP[1]

By Karl Fischer

SUMMARY

The investigation of the flow in a centrifugal pump indicated that the flow patterns in frictional fluid are fundamentally different from those in frictionless fluid. In particular, the dead air space adhering to the section side undoubtedly causes a reduction of the theoretically possible delivery head.

The velocity distribution over a parallel circle is also subjected to a noticeable change as a result of the incomplete filling of the passages. The relative velocity on the pressure side of the vane, which for passages completely filled with active flow would differ little from zero even at comparatively lower than normal delivery volume, is increased, so that no rapid reverse flow occurs on the pressure side of the vane even for smaller delivery volume.

It was established, further, that the flow ceases to be stationary for very small quantities of water.

The inflow to the impeller can be regarded as radial for the operating range in question.

The velocity triangles at the exit are subjected to a significant alteration in shape as a result of the increased peripheral velocity, which may be of particular importance in the determination of the guide vane entrance angle.

---

[1] "Untersuchung der Stromung in einer Zentrifugal-Pumpe." Mitteilungen des Hydraulischen Instituts der Technischen Hochschule, München, No. 4, 1931, pp. 1-27.

INTRODUCTION

The actual power input of a centrifugal pump is considerably less than that stipulated theoretically on the assumption of an infinite number of vanes. The cause of the power reduction lies in the uneven pressure and velocity distribution over a parallel circle as consequence of the "passage vortex." It is true that the modern calculating methods allow for this phenomenon and also for the reduction in flow-off angle directly connected with it, and do achieve a satisfactory agreement with reality by means of correction factors. Nevertheless, the velocity triangles at the exit, which are decisive for the attainable delivery heads, cannot be definitely indicated. Exact knowledge of the flow conditions especially at the exit is, on the other hand, desirable in many respects, such as in the design of the guide vanes, for instance. The assumptions which are necessary for the prediction of the flow pattern, especially the one that the impeller passages run always full with active flow, lead to erroneous conceptions of the flow distribution, particularly for smaller throughflow quantities, as will be readily seen from the subsequent report. Admittedly, there was no longer any doubt as to the incorrectness of the assumption of passages being completely filled with active flow, after the phenomenon of dead air space formation on airplane wings had been closely observed. But little importance was attached to this fact in its effect on the performance.

Theoretical studies of the extent of this effect introduced by the formation of dead air space present considerable difficulties, because of the absence of any kind of reference data on the extent of the dead air zones and their variability with changes of $\frac{q}{\omega}$ (q = throughflow quantity, ω = angular velocity). The experimental investigation of these phenomenona with the use of the rotoscope (devised by D. Thoma) forms the subject of the present report.

DESCRIPTION OF THE EXPERIMENTAL SETUP

The posed problem of exploring the flow processes in a centrifugal pump demanded that the principal aim in the structural design of the experimental pump be centered on the possibility of clear observation of the flow.

Experimental Pump (Fig. 1).

The water system differed little from standard practice, except that the arrangement and the drive of the pump were designed for the particular purpose in view. By arrangement of the impeller conforming to figure 1, the section pipe became stationary, and the observation of the flow was not obstructed by an extraneous support. It is essential that the impeller be shut off in front by a glass wall.

Impeller

The impeller has six vanes of conventional design. For constructive reasons the vanes were of 8-millimeter thickness. The impeller was designed for $n = 400$ rpm, $Q = 8.3$ liters per second, and $H = 1.65$ meters.

The principal dimensions are as follows:

Width at entrance	$b_1 = 0.0225$ meter
Width at discharge	$b_2 = 0.020$ meter
Diameter at entrance	$D_1 = 0.140$ meter
Diameter at discharge	$D_2 = 0.280$ meter
Diameter of inlet pipe	$D_s = 0.100$ meter
Number of vanes	$z = 6$
Entrance angle	$\beta_1 = 17^\circ$
Discharge angle	$\beta_2 = 28^\circ$

The impeller was illuminated by six concentrically arranged 100-watt lamps. For the photographic work six arc lamps of about 1000 candle power each were added, which reduced the exposure time to 1/1000 second.

Total Arrangement

The water taken from a pressure line was carried to the test pump by way of a large water tank kept at constant level by an overflow. The whole arrangement can be seen from figures 1, 3, and 4. Pressure and water were regulated by a slide valve fitted in the pressure line. From there the water passed to the balance set up in the subcellar where it was discharged in the tail water after weighing. The pump was driven by electric motor with variable speed. In order to eliminate the viscosity effect, which is much more evident at the comparatively small dimensions of the test pump, than

in most practical applications, the speed was chosen as high as consistent with the strength of the glass plate — 450 rpm. The Reynolds number is, of course, occasionally greater in practical applications; for normal water volume and n = 450 rpm the Reynolds number of the test pump referred to the hydraulic radius at the inlet and outlet of the impeller passages, was, however, 164,000 and 108,000, so that no fundamental changes of the flow are to be expected for larger versions.

The head was measured by mercury manometer.

Observation of Flow

The flow is observed during the operation of the pump by the rotoscope shown in figures 1 and 4. The rotoscope (reference 1) is based on the phenomenon that the reflected image of a stationary object rotates when the plane of reflection is rotated.

Therefore, it is possible to make a rotating object appear at rest when the object is reflected about a plane which passes through the line of view coinciding with the axis of rotation and rotates at half the impeller speed about the line of vision. The reflection is affected by a so-called Dove prism. The rotoscope, set up 1.2 to 1.5 meters from the pump impeller, is driven by belt and electric motor; a fly wheel takes up minor irregularities of the drive. The speed is adjusted by series resistance and braking of the fly wheel by hand to half pump speed. The rotoscope gives a perfectly still picture only when it is mounted co-axially with the pump. In many tests, however, a camera rotating at pump speed was arranged instead in the extension of the pump center, bringing its optical axis on a line with the pump shaft. The camera was operated by chains and countershaft from the pump. The shutter was released during operation. An interconnected, electrically actuated friction coupling permitted starting and stopping of the photographic apparatus (interruption of rotary motion) without having to stop the pump. (See fig. 6.) But for the photographing the rotoscope was utilized at the same time, because it is not necessary in all circumstances that pump shaft and rotoscope axis coincide in one line. Even when both meet at not too great an angle, satisfactory observations are still obtainable for many purposes, so long as this point of intersection coincides with the center of the impeller (fig. 7). The use of camera and rotoscope simultaneously has the great advantage of accurate timing of the flow attitude desired for photographing.

The flow was rendered visible by a mixture of azo-acid (red) and nigrosine introduced at various points, indicated as A, B, and C. The dye was introduced centrally through a 5-millimeters thick brass tubing (rotating) in the pump shaft (fig. 1). To forestall accidental disturbances due to the finite thickness of the dye tubes (2-millimeter thickness) one vane was equipped with three holes (0.5 millimeter in diameter) into which the dye was poured through a covered groove in the vane (fig. 8). The speed of outflow was kept low by suitably chosen height level of the dye container, in order to avoid a falsification of the flow pattern through high entrance speed of the dye mixture.

EXPERIMENTAL RESULTS

Note: According to the investigations by Oertli (reference 2) in the laboratory of the Federal University, Zürich, the flow through a centrifugal pump is not completely two-dimensional, although he was able to establish the fact that, except for unusually wide departure from normal operating conditions, the total flow in the impeller is sufficiently characterized by the distribution of the stream filaments in the median throughflow plane. For this reason the dye outlet flow was arranged in the center of the vanes.

Inflow to Impeller

In order to obtain information regarding the assumption of vertical inflow serving as basis of the impeller calculation, the observation of the absolute flow became necessary. Hence, in these experiments the rotoscope and the rotating camera were not required. The observation was made by naked eye, the photographic records were made by stationary camera. Five different flow attitudes for $n = 450$ rpm are reproduced in figures 9, 10, 11, 12, and 13. The corresponding photographs from test series II ($n = 350$ rpm) show no difference in flow distribution from those taken at $n = 450$ rpm.

Figure	rpm	Q (liters/sec)	$\frac{Q}{Q_{norm}}$	H (m)	Remarks
9	450	14.81	1.58	0.752	Q above normal
10	450	9.40	1.00	1,885	Q normal
11	450	5.74	.61	2.351	Q below normal
12	450	3.20	.34	2.568	Q below normal
13	450	1.85	.20	2.589	Q below normal

It is readily seen that the departure from vertical inflow remains within narrow limits. "Preliminary rotation" becomes perceptible only for small quantities of water (figs. 12 and 13). This is likely to be due less to friction effect than to reverse flow from the impeller passages, which, at sinking of the delivered water volume below a certain limit, was very plainly observed in the subsequently described tests (fig. 19). For the present, it may be stated that reverse flow begins in several passages at greatly subnormal water volumes, but that the flow is not stationary in respect to the impeller. The place at which the reverse flow prevails, varies. The back flowing water subjected to rotation mixes in the space before the entrance with the fresh water and causes it to rotate. The mixing process combines with the reverse flow to produce a very irregular velocity distribution, as exemplified in the peculiarly torn and twisted form of the dye filament. (See figs. 12 and 13.)

Flow in the Impeller Passages

A number of theoretical studies have dealt with the problem of identifying the relative flow in rotating channels. The procedure usually consisted of dividing the total flow into two parts, a vortex free throughflow and a flow with constant vortex corresponding to the angular velocity of the impeller, but without throughflow. The great advantage of such a division is that the variations in the velocity conditions at changes in throughflow or angular velocity are easily accounted for. Kucharski (reference 3) succeeded, although with friction discounted, in finding a rigorous theoretical solution for a rotating impeller of very simple form with straight vanes of finite length reaching radially to the center. The conventionally employed impeller forms with curved passages, finite vane lengths, which intersect the entrance circle, offer considerable difficulties to the mathematical solution of the flow pattern. In this connection reference is made to studies by Spannhake (reference 4) which were made by means of conformal transformation on the basis of specific conditions. But the actually resulting flows, especially for very small quantities of water, departed considerably from the theoretical solution on account of the friction and the instability and separation phenomena induced by it. From the observations described here it was concluded that in no case, whether at normal, above, or below normal delivery of water, the passages were completely filled with active flow.

Determination of limit between dead air space and active flow.- For reasons of greater accuracy in the subsequent investigations the dye outlet designated with A is largely resorted to. At the start of the dye injection the boundary layer emanating from the entrance edge is, at first, considerably colored, as seen from figure 14 (dye inflow at B) taken a short time after start of dye outflow. The coloring of the dead air space is barely noticeable. But gradually the color collects in the dead air space until finally the entire space appears filled with colored liquid (cf. fig. 16). Apart from small and very small quantities of water, a fairly sharp separation appears to take place. This is not to imply, however, that no interchange of fluid occurs at all between the two zones. (The preservation of the vortex motion specifies an interchange.) But, in general, the amount of water that passes through the dead air space is disappearingly small compared to the total delivery.

Description of flow at different proportions of water volume $\frac{Q}{Q_{normal}}$.- The decrease of the ratio $\frac{Q}{Q_{normal}}$ below a certain limit is accompanied by two typical characteristics in the flow:

1. The flow is no longer stationary (appearance of varying reverse flows).

2. The flow attitude at a given time interval differs in the several impeller passages.

The transition from stationary to pulsating flow is illustrated on several worked-out problems.

In figure 15 the flow conditions are represented for

$n = 252$ rpm; $Q = 2.46$ liters per second

$\frac{Q}{Q_{normal}} = 0.47$; $H = 0.75$ meter

(Graphical reproduction of relative flow observed in the rotoscope.) No dissimilarity of flow conditions were observed in the individual impeller passages for this quantity of water, but more than half of the passages were full of dead air. The active zone was only a fairly narrow strip closely hugging the pressure side of the vane. A brisk vortex motion prevailed in the dead air zone.

Figure 16 is the photographically obtained flow picture for $n = 250$ rpm; $Q = 2.79$ liters per second; $\frac{Q}{Q_{normal}} = 0.53$; $H = 0.77$ meter.

Figure 17. The water performance was reduced to 1.038 liters per second $\left| \frac{Q}{Q_{normal}} = 0.206; \quad n = 240 \text{ rpm}; \quad H = 0.79 \text{ meter} \right|$.

This condition is characterized by fairly regularly recurring pulsations (1.5-sec periods). The inflow to the impeller passages itself is no longer regular. The source of these disturbances lies undoubtedly with the impeller vanes. The impeller passages are now almost completely filled with dead air which pulsates periodically. The forward and backward flow in the passages is not simultaneous; but while the water flows forward in several passages, it flows back in others. During the return flow a part of the passage content spills over the entrance circle again and so passes into the next or next to the next passage. The water particles of the effective water current are probably conveyed intermittently through the impeller passages at the individual periods.

The exact process within a period is described with the aid of figure 17 ($Q = 1.038$ liters per second; $n = 240$ rpm; $\frac{Q}{Q_{normal}} = 0.206$; $H = 0.79$ meter). The color jet emerges (beginning of period) at point B and runs along the pressure side (fig. 17, first condition) in channel I for a short distance while closely adhering, then begins to form vortices under gradual separation from the vane wall, which fill the entire width of passage I. The time during which the color jet enters this passage amounts to a small fraction of a second. The color vortices, however, remain for a comparatively long time in the passage and pulsate back and forth. A gradual break-away of the colored water particles occurs at point a on the vane. In the meantime the principal flow has formed in passage II (fig. 17, second flow condition), approximately 1/3 to 1/4 second after start of the period. The color jet proceeds as indicated and forms vortices which nearly fill the entire passage. These vortices likewise pulsate back and forth, while the vane tip at 6 manifested break-away of colored water particles. The termination

of the forward flow in passage II is indicated by a sudden inflow of colored water into passage III (fig. 17, third flow condition), where the same phenomena were observed as a short time before in passages II and I. This is the end of a period, during which the impeller makes from 5 to 7 revolutions.

Figures 18 and 19. The photographs need no further explanation. Reverse flows in the passages I and IV are plainly visible, likewise the forward flow of the water in passage III. Figure 20 ($n = 243$ rpm; $Q = 0.133$ liters per second; $\frac{Q}{Q_{normal}} = 0.025$; $H = 0.812$ meter). The irregularities of the flow are more pronounced, since the pulsations are more active and the area in which these motions occur is greater.

In connection with the description of flow conditions for different below-normal quantities of water, several photographic records have been included although they offer nothing new in principle. For these photographs a different coloring method was used at the suggestion of D. Thoma. Through a valve mounted in the suction pipe of the test pump, which received the dyestuff under positive pressure, it was possible occasionally to color the total delivery water. At the start of the test the pump was driven with clear water. The valve was opened shortly before releasing the shutter. The active flow shows up black in the flow pictures (figs. 21 and 22), while the dead air spaces on the suction side of the vane are still filled with clear water.

With larger volumes of water the coloring of the total delivery water became impractical for the identification of the two zones, because the interchange of colored and clear water was too rapid in consequence of brisk turbulence; hence the photographs did not turn out satisfactory. Better results were obtained with a partial coloration of the water. This was secured by a dividing wall in the suction pipe of the pump, with the valve in the position shown in figure 23. The vanes passed alternately in a zone of dyed and clear water. The dead air spaces in the upper part of the picture again appear as black areas (fig. 24). $\frac{Q}{Q_{normal}} = 0.47$.

Flow at normal water volume $\left(\frac{Q}{Q_{normal}} = 1\right)$.- Figure 25 represents the flow conditions for $n = 400$ rpm; $Q = 3.86$ liters per second; $\frac{Q}{Q_{normal}} = 1.05$; $H = 1.41$ meters.

The first premise of a hydraulically beneficial flow – shock free entry – is complied with as can be deduced from the clearage of the dye filament at point B. (The mouth of the coloring tube was located in the extension of the median line of the vane.) Contrariwise, it is found that the flow in the impeller passages is not quite as desired. A dead air space clings to the suction side of the vane at the exit, which for the area available for the throughflow reduces the section Z–Z by about 1/3, and consequently raises the velocity of the water by 50 percent. This formation of dead air space causes a flow-off at a much smaller angle than the vane exit angle (20.5° as against 28°). There was scarcely any evidence of separation at the pressure side of the vane. The flow hugs the vane wall closely.

Relation between the Dead Air Spaces on the Suction and Pressure Side of the Vane at Variation in Throughflow Volume

The findings of the preceding two chapters are now briefly summarized in order to point out the variations of the resultant flow pattern on changing from one volume of water to another. The observations indicated that even for supernormal water volume a dead air space develops at the outlet on the vane suction side, which on reduction of the delivered volume increases in extent. The break-away point shifts continuously toward the entrance edge. On the pressure side the phenomena are reversed. The dead air space, which is greatest for supernormal volume of water, decreases and disappears altogether for normal or subnormal volume. The passage cross section available for the active flow then is governed by the extent of the suction side dead air space. If the volume of water is small the active flow is restricted to a small passage along the pressure side of the vane, a phenomenon which is not to be expected in frictionless fluid.

To gain an insight into the magnitude, extent, and variation of the dead air spaces, as well as their relationship, it was necessary to include the flow pictures of the other rotational speeds for the interpretation (fig. 27). The lines of demarcation between active zone and dead air space were determined from the photographic records. The very nature of the matter made a sharp definition of the boundary lines of the two areas impossible. The intermingling is much more pronounced for small volumes than for great

volumes. The plotting of the four employed speeds condensed in figure 27 indicates that the boundary areas between active flow and dead air space on suction and pressure side of the vane diverge very little for any delivery volume (very small quantities of water excepted). In other words, the passage remaining for the active flow between inlet and discharge cross section has nearly the same width. When the dead air space at the pressure side disappears the boundary area runs approximately parallel to the vane.

COMPARISON OF THE FLOW PATTERNS OF FRICTIONLESS FLUID WITH THE OBTAINED FLOW PICTURES

Since the resultant flow in frictionless fluid can be regarded as being composed of two unrelated separate flows (pure rotation flow with the passage vortex ω and the throughflow) the character of the total flow is on the whole determined by the rotation flow when the quantities of water are small $\frac{Q}{\omega}$ = small, and by the throughflow when the quantities of water are great (supernormal).

Pure Rotation Flow Q = 0

The flow pattern represented in figure 28 for pure rotation flow (Q = 0) was computed by Kucharski for the straight radial vane extending to the center. Applied to the present impeller conditions the flow pattern should be as shown in figure 29 (operation in frictionless fluid.) The fluid circles relative to the impeller passage in closed orbits about a stationary nucleus. A comparison with the conditions of flow in figures 30 and 31 indicates that the presence of friction introduces a fundamental change in the character of the pure rotation flow. The negative passage vortex is dissolved in a number of continuously changing single vortices, without a trace of the original existence of the negative passage vortex. However, this deviation should not be held as objection against the theory, because it is clear that the friction attains controlling influence for deficient throughflow—or more precisely for very small throughflow—covering only the slot losses. At most, the theoretical flow pattern might be expected immediately after starting.

Flow at Small Quantities of Water

Kucharski's theoretical prediction of the flow pattern in frictionless fluid (fig. 32) affords a reference point for plotting the streamlines for the present impeller conditions (fig. 33).

The separation of a fluid core on the pressure side of the vane is unusual. For small quantities $\left(\frac{Q}{Q_{normal}} = \text{small}\right)$ the velocities caused by the passage vortex exceed the pure throughflow velocity; thus reverse flows are to be expected on the pressure side of the vane, where the velocities are subtracted. Contrariwise, the velocity increases at the suction side of the vane. The operation in frictionless fluid presents no occasion for continuously changing, dissimilar flow conditions in the individual impeller passages, in point of fact the same condition, which remains constant for a certain operating case, will prevail in all passages.

The flow picture of figure 15 serves for comparison; its delivery is surely reduced to such an extent that in frictionless fluid reverse flows are to be expected on the pressure side of the vane, while the uncertainties, introduced by the pulsation of the flow for very small quantities of water, are removed. The following picture is presented: Reverse flows on the pressure side of the vane in consequence of the negative passage vortex do, in fact, not occur, rather a substantial dead air space develops on the suction side of the vane.

EFFECT OF DEAD AIR SPACE ON THE OBTAINABLE HEAD

The decrease in the power absorption of an impeller is partly explained by the described processes.

The principal equation, under the assumption of vertical inflow and infinite number of vanes, gives the theoretical head (fig. 34a) at

$$H_{th} = \frac{1}{g} c_{2u} u_2$$

In figure 34b the average velocity triangle at the exit is shown as obtainable on the premise of finite number of vanes and with pressure and velocity distribution over a parallel

circle according to data in literature (reference 5) (complete filling of passages with active flow presumed). Qualitatively, the calculation furnished a correct picture; the actually occurring velocities on the pressure and suction side of the vane can be seen from figure 35. The relative position of the colored filaments affords an insight into the velocity distribution of the impeller. In the same time interval, during which particle P travels the distance PP", the water particle Q reaches Q". This distance is much shorter, hence proves the higher speed on the suction side of the vane. This phenomenon increases the average relative discharge velocity and reduces the outflow angle; both result in a reduced power absorption. The incomplete filling of the impeller passages with active flow acts in the same sense; it produces a further increase in the average relative discharge velocity and a second reduction of the head. (Cf. velocity triangle, fig. 34c.)

EFFECT OF INCREASED MERIDIAN VELOCITY c'_{2m} ON THE SIZE OF THE GUIDE VANE ENTRANCE ANGLE

The absolute paths of the water particles after exit from the impeller are, theoretically, logarithmic spirals on the assumption of constant width of passages. The dissimilarity of angle α and α' is evident from figure 34. The tangent of angle α' under which the absolute paths slope toward the circumference is

$$\tan \alpha' = \frac{c'_{2m}}{c_{2u}}$$

It is seen that the increase from c_{2m} to c'_{2m} caused by the dead air space produces a greater angle α'. With angle α, the active flow would result in a shock at the impeller entrance. The existence of the clearance space between impeller and guide apparatus lessens, the entrance shock because a certain equalization is achieved in this part.

EFFECT OF GUIDE APPARATUS ON THE RELATIVE FLOW IN THE IMPELLER

The presence of a guide apparatus itself affects the flow in the impeller. The relative flow in the impeller loses its stationary character. This phenomenon ties in with the too-

small guide vane entrance angles — owing to nonobservation of the dead air space formation. The flow-off conditions for the separate flow tubes of a passage differ at a specific instant. At point A (fig. 36) only a small space is available to the flow for a change in direction; hence the shock is relatively stronger than at B. The flow pictures indicate that the presence of a guide apparatus can, under certain circumstances, become the cause of new disturbances. The experience of several researches (reference 6), that the installation of a guide apparatus improves the efficiency only for very accurately chosen guide vane entrance angles, is herewith explained.

Translation by J. Vanier,
National Advisory Committee
for Aeronautics.

REFERENCES

1. Thoma, D.: Die Versuchsanstalt für Wasserturbinen in Gotha. Gotha 1918, Verlag Engelhardt-Reyher.

2. Oertli, Heinrich: Untersuchung der Wasserströmung durch ein rotierendes Zellenkreiselrad. Lab. Zürich.

3. Kucharski: Strömungen einer reibungsfreien Flüssigkeit bei Rotation fester Körper, München 1918.

4. Spannhake: Hydraulische Probleme, Mitteilungen des Instituts für Strömungsmaschinen der Technischen Hochschule Karlsruhe No. 1, 1930.

5. Pfleiderer, C.: Die Kreiselpumpen, Berlin 1924. p. 89.

6. Omori, Tokusaka: Experimental Researches on Centrifugal Pumps.

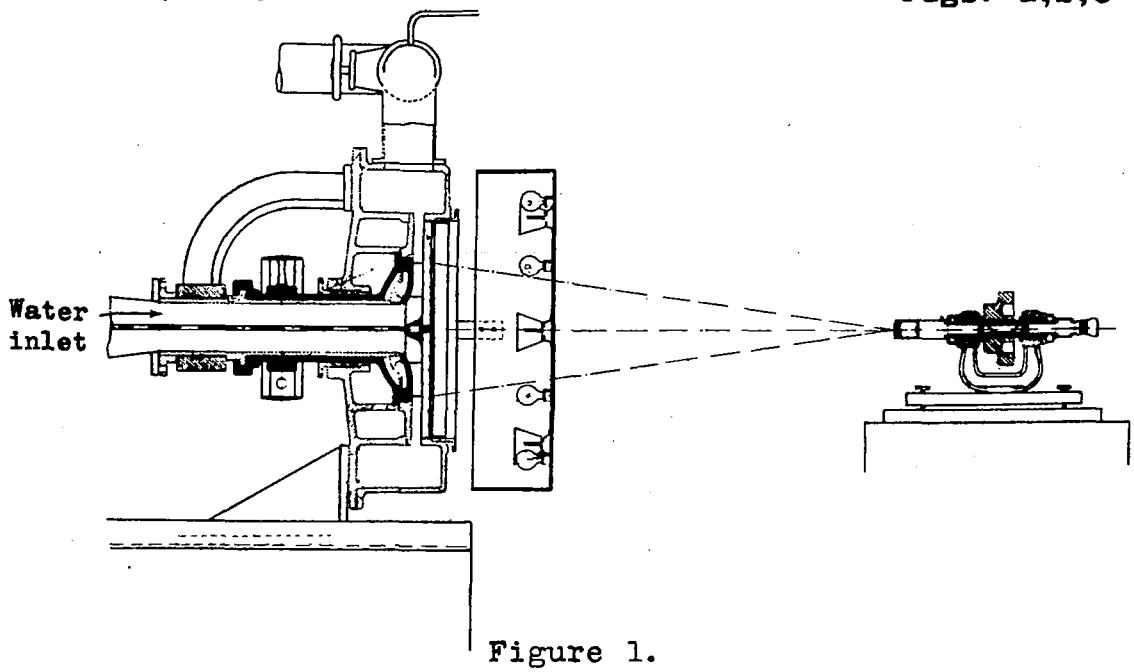

Figure 1.

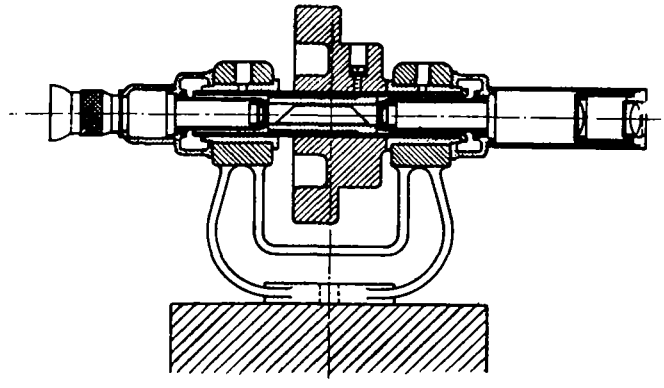

Figure 2.

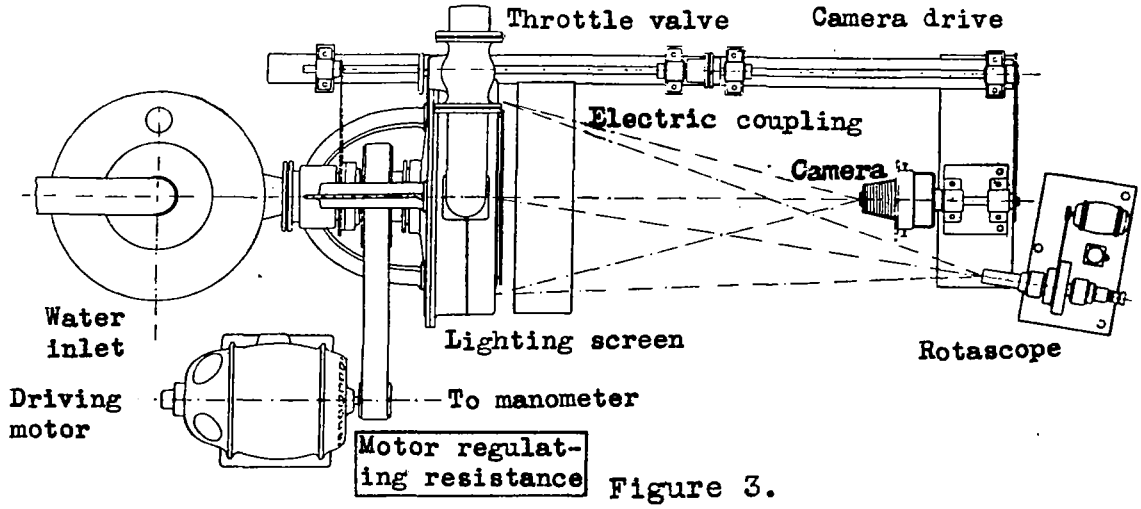

Figure 3.

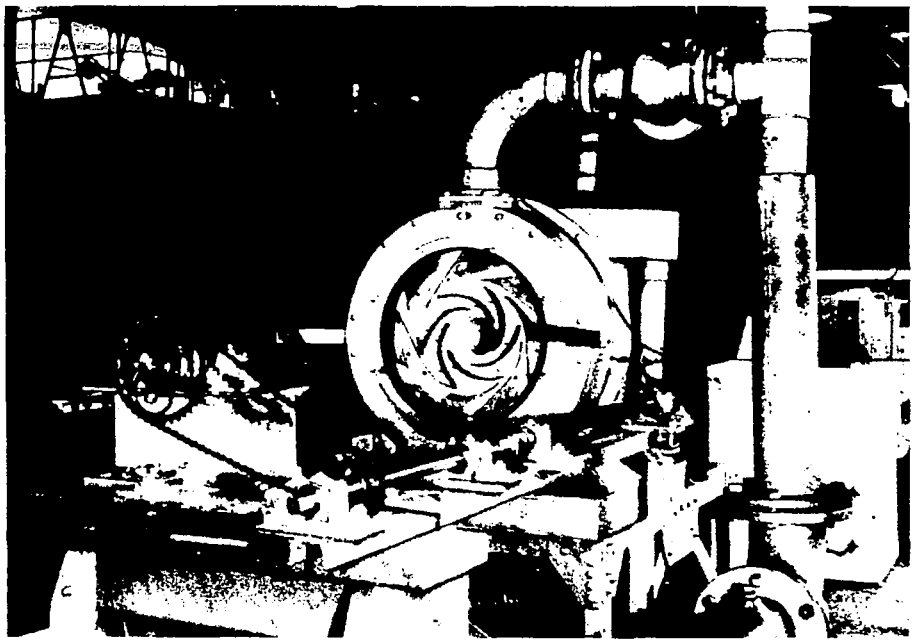

Figure 4.

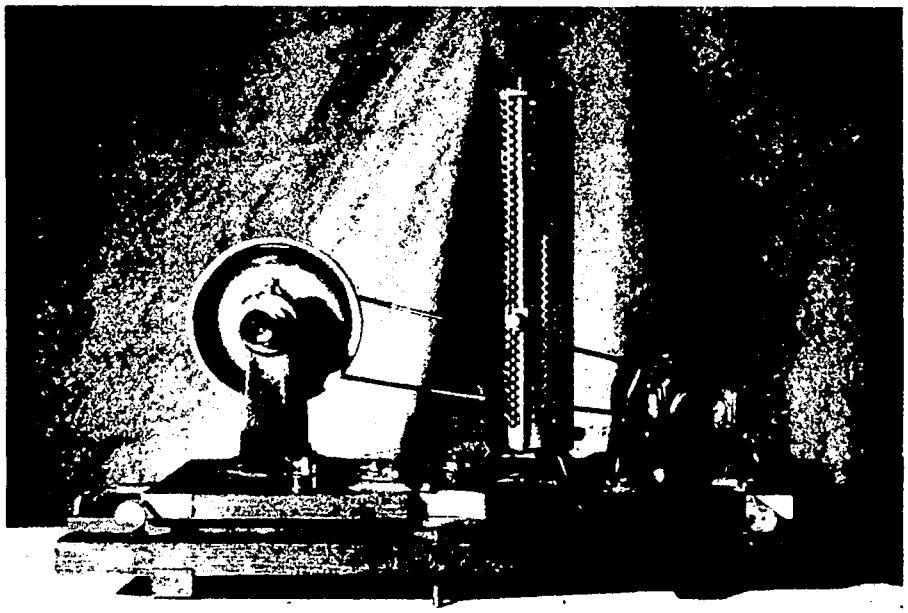

Figure 5.

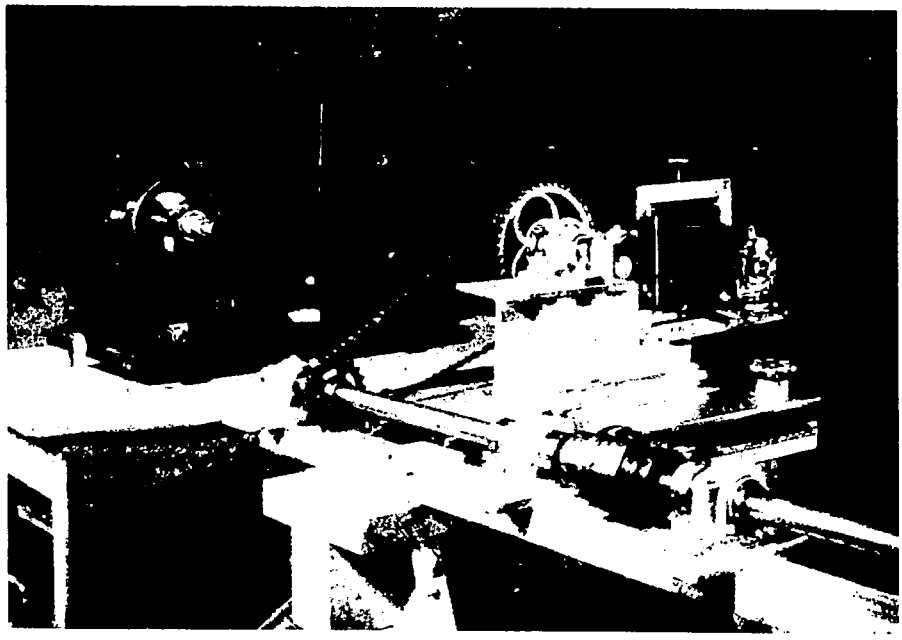

Figure 6.

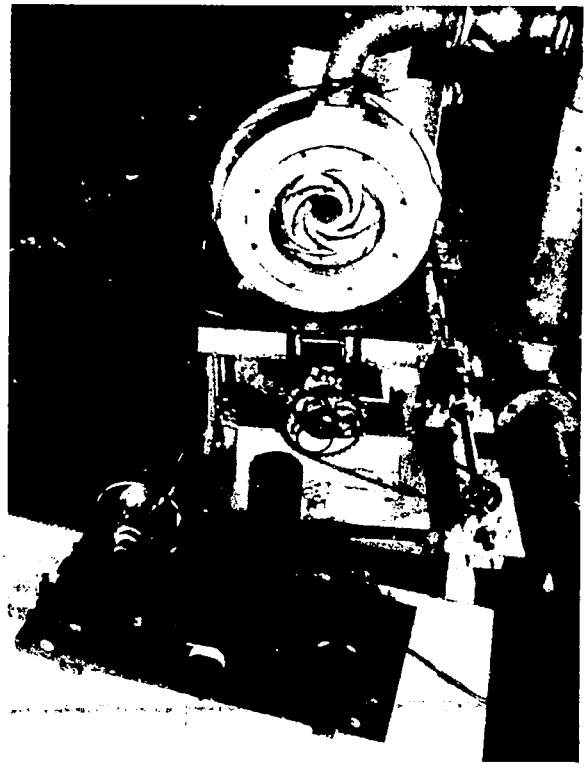

Figure 7.

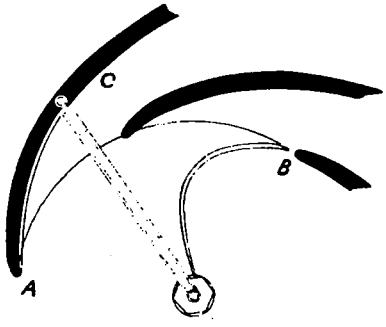

Figure 8.

Figure 9.

Figure 10.

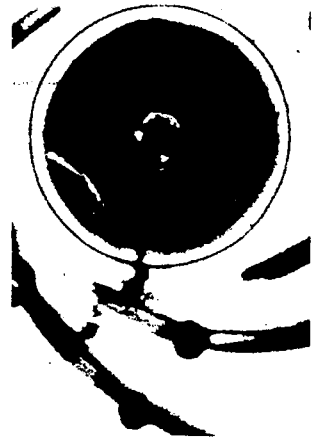

Figure 11.

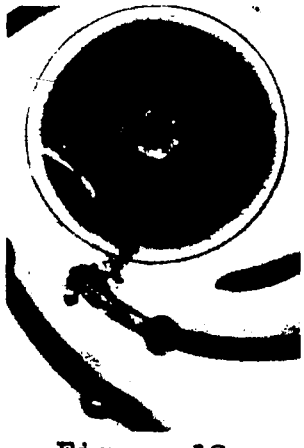

Figure 12.

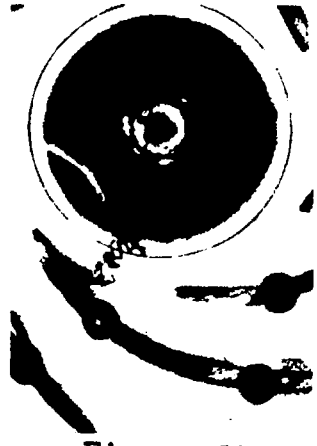

Figure 13.

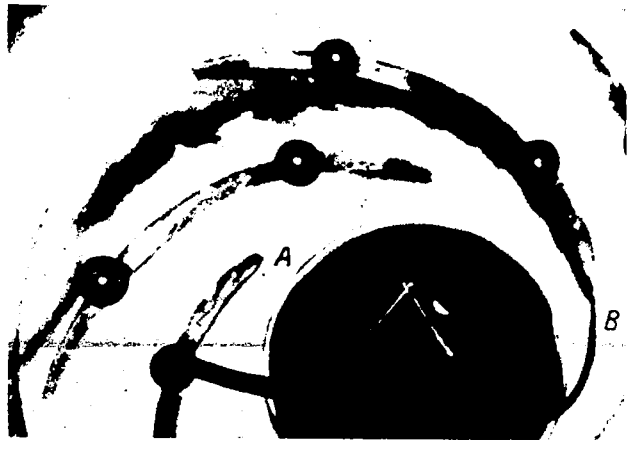

Figure 14.

Figure 15.

Figure 16.

(1) Condition

(2) Condition

(3) Condition

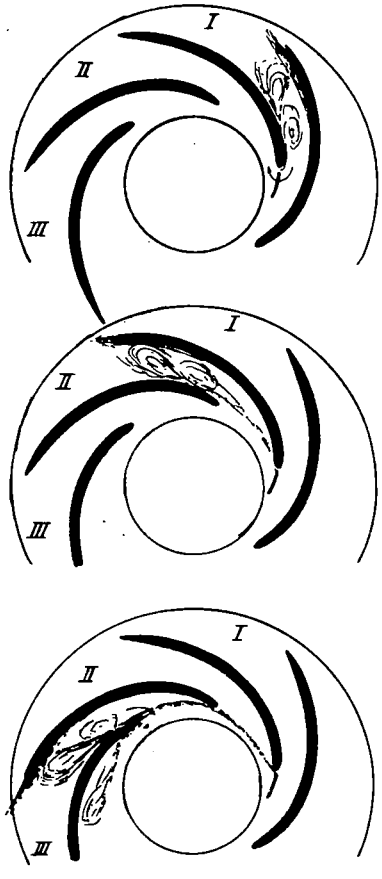

Figure 17.

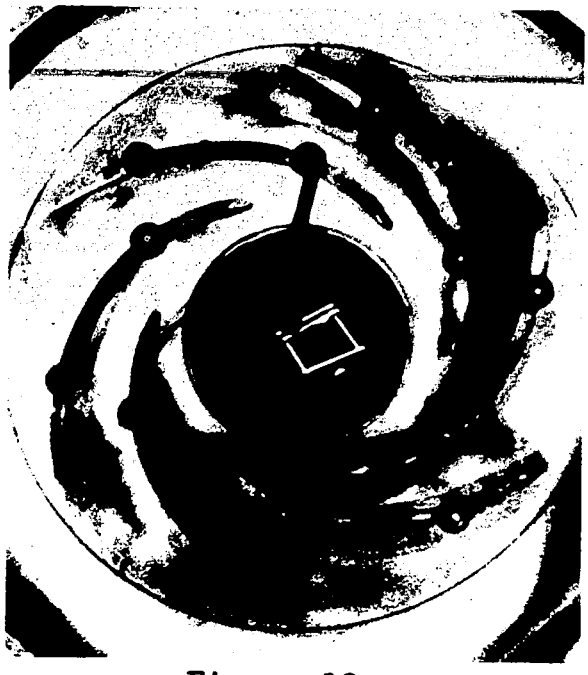

Figure 18.

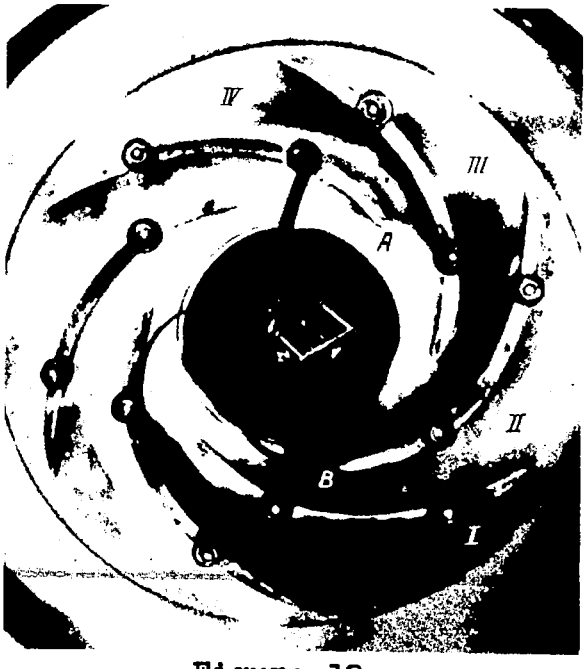

Figure 19.

(1) Condition

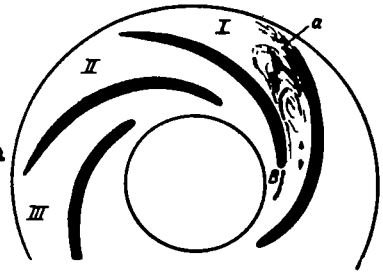

(2) Condition

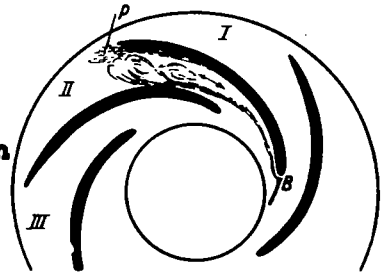

(3) Condition

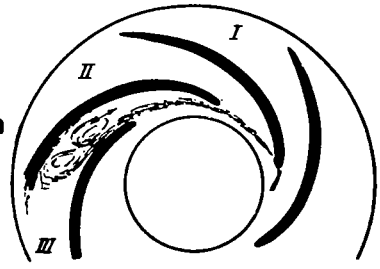

Figure 20.

Figure 21.

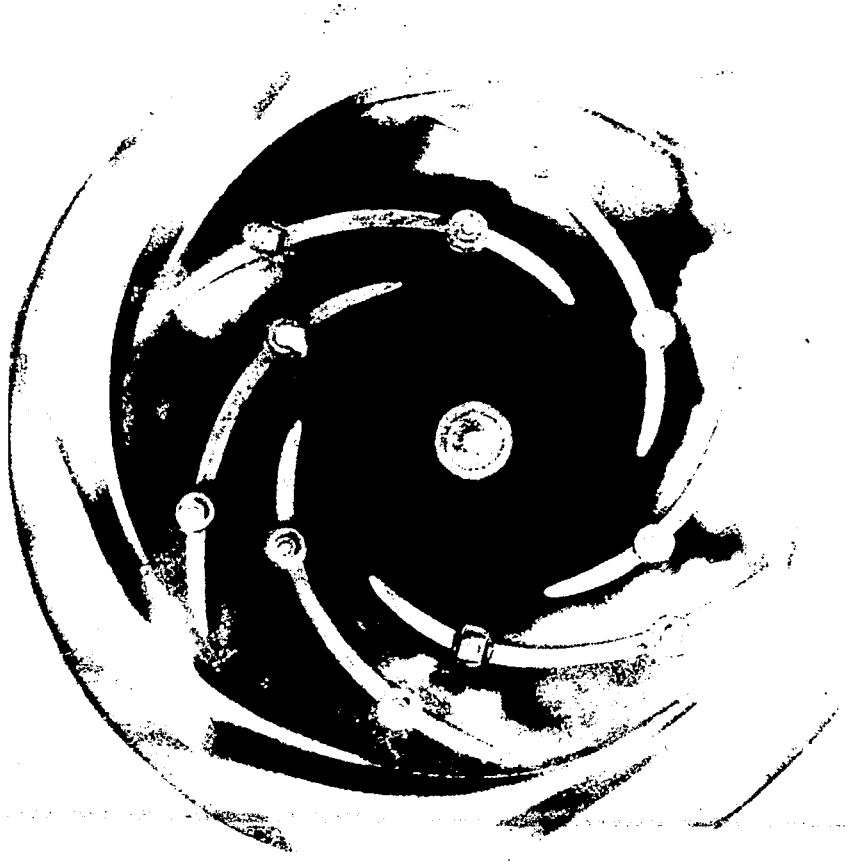

Figure 22.- Frontispiece: separation of flow in a centrifugal pump at 400 rpm; made visible by sudden coloration of inflowing water. Subnormal quantity of water; taken with rotating camera; exposure: 1/250 sec.

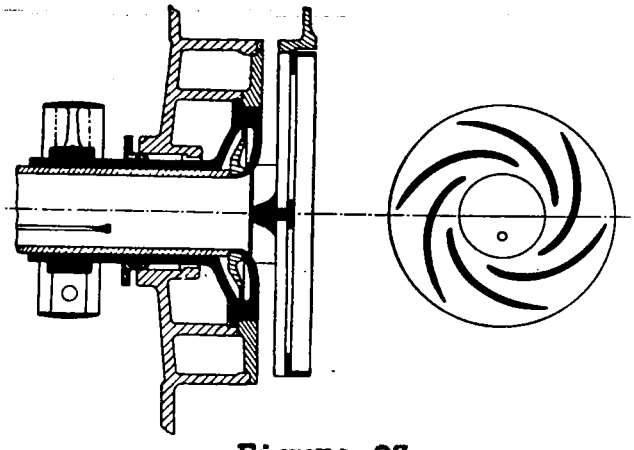

Figure 23.

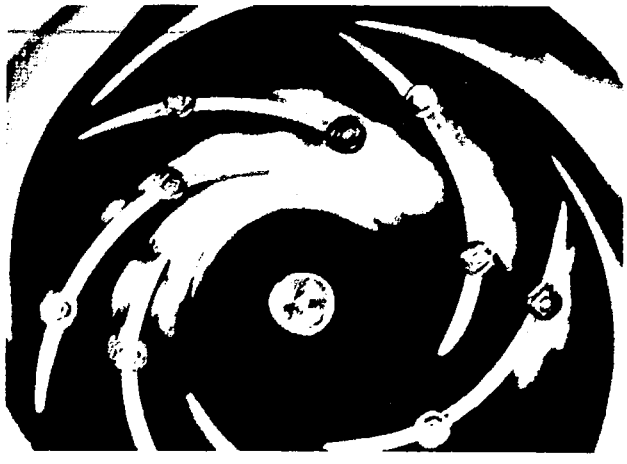

Figure 24.

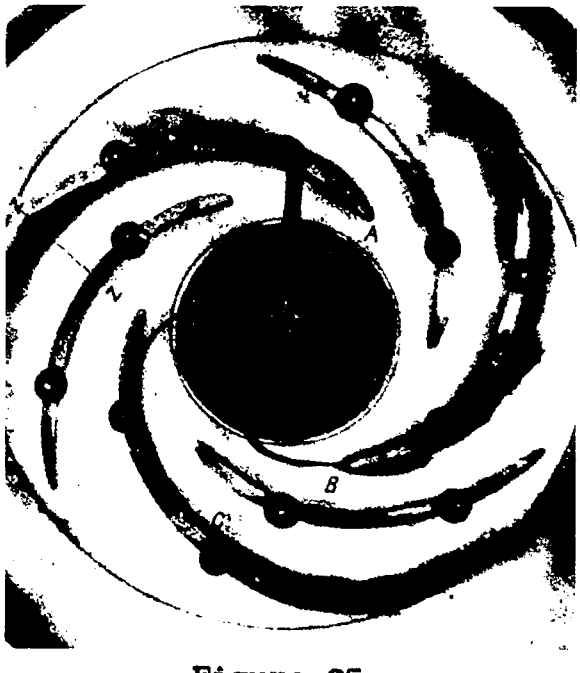

Figure 25.

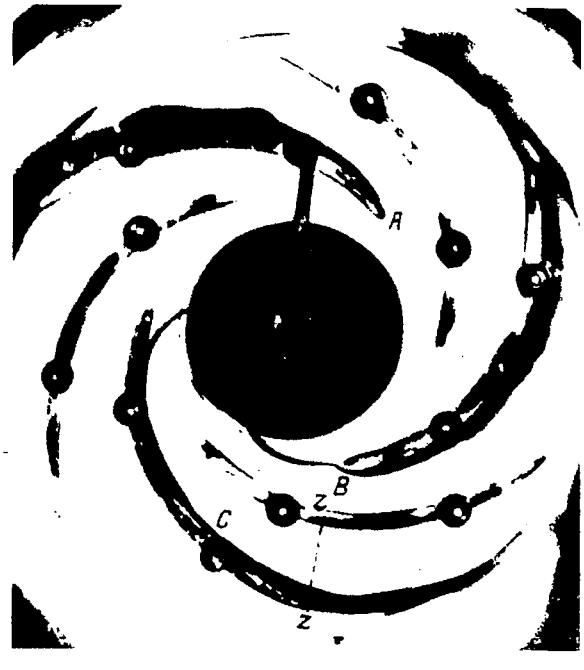

Figure 26.

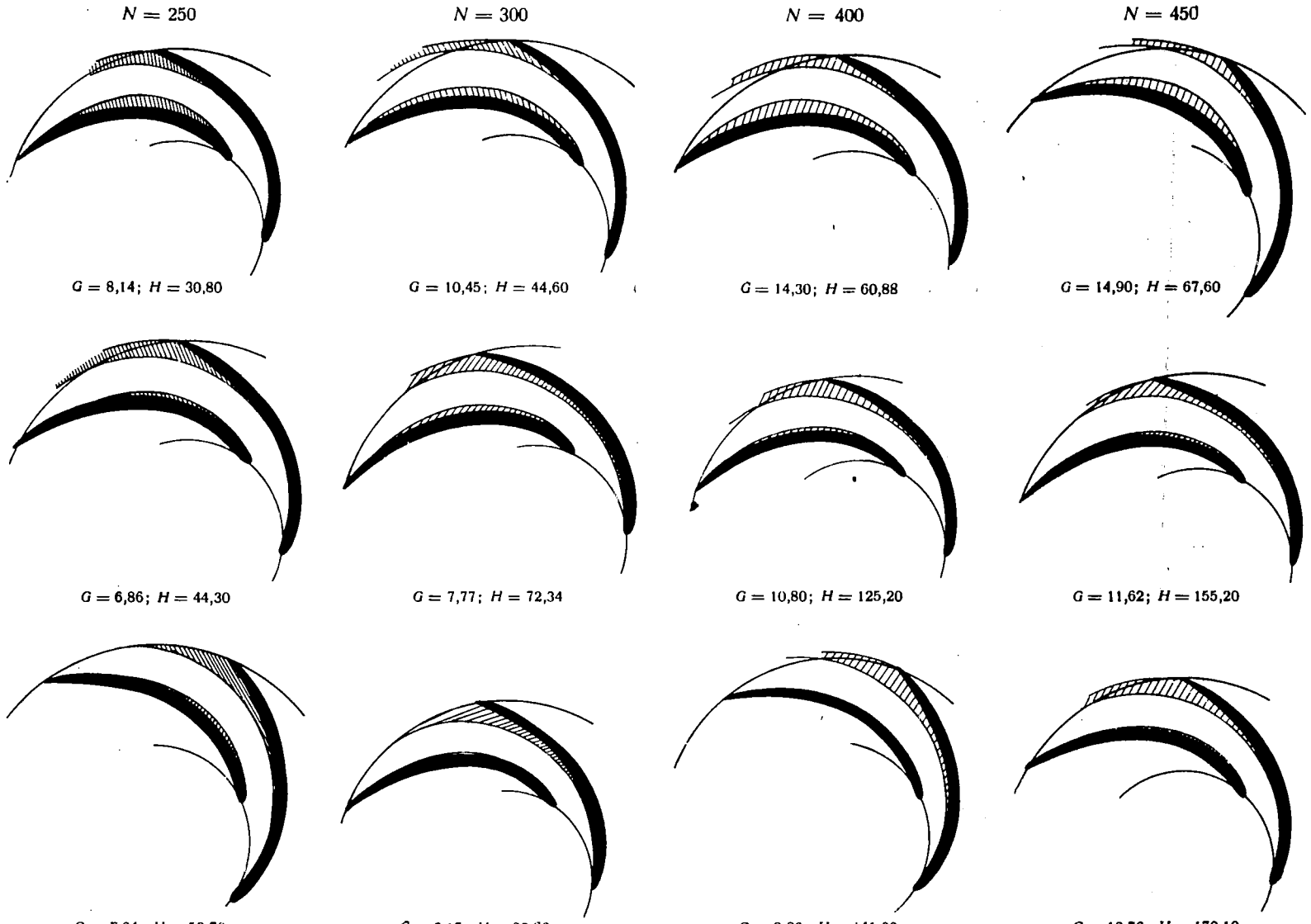
N = 250
N = 300
N = 400
N = 450
G = 8,14; H = 30,80
G = 10,45; H = 44,60
G = 14,30; H = 60,88
G = 14,90; H = 67,60
G = 6,86; H = 44,30
G = 7,77; H = 72,34
G = 10,80; H = 125,20
G = 11,62; H = 155,20
G = 5,94; H = 52,70
G = 6,17; H = 92,80
G = 8,86; H = 141,00
G = 10,76; H = 170,10

Figure 27.

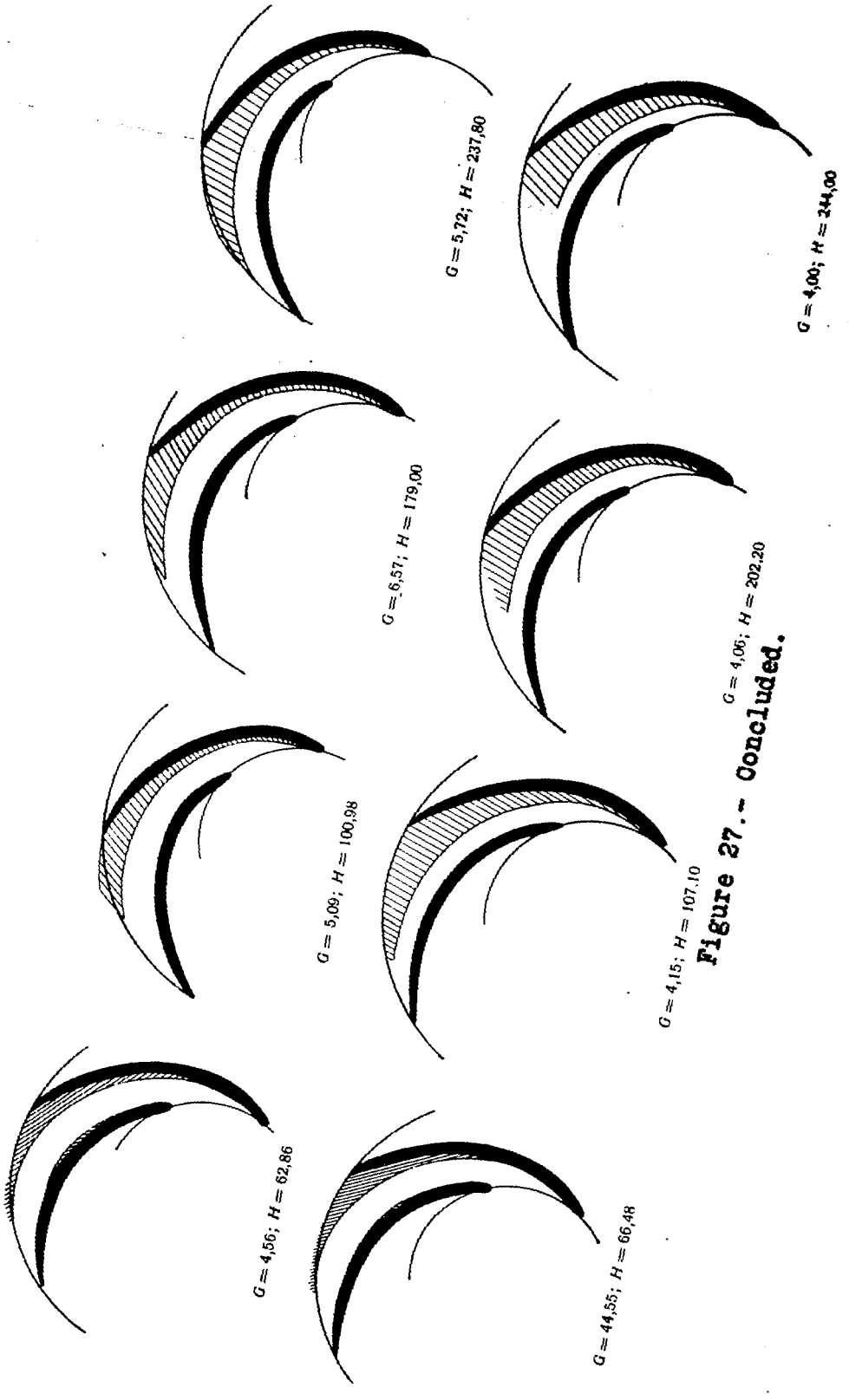

Figure 27.- Concluded.

Fig. 27b

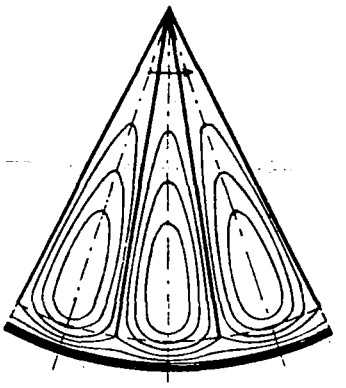

Figure 28.

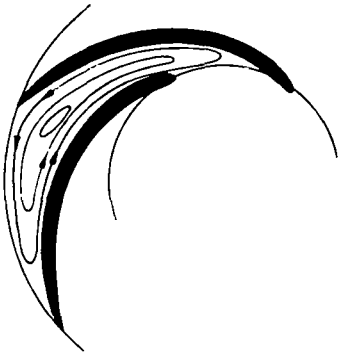

Figure 29.

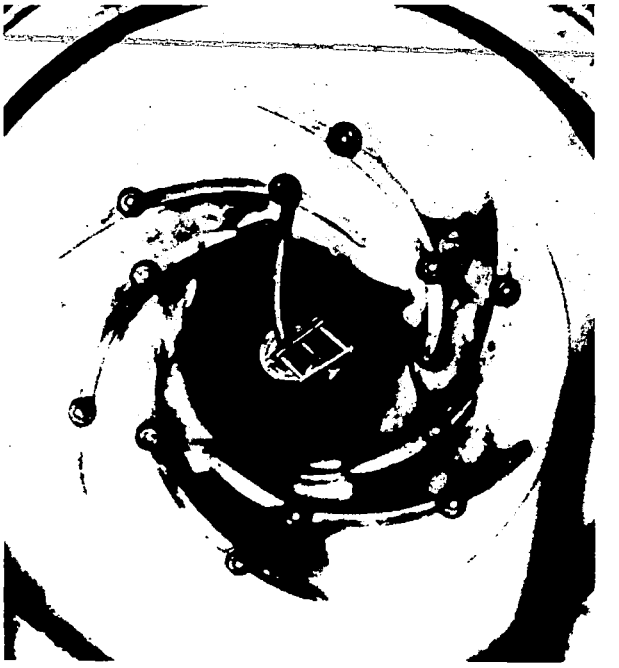

Figure 30.

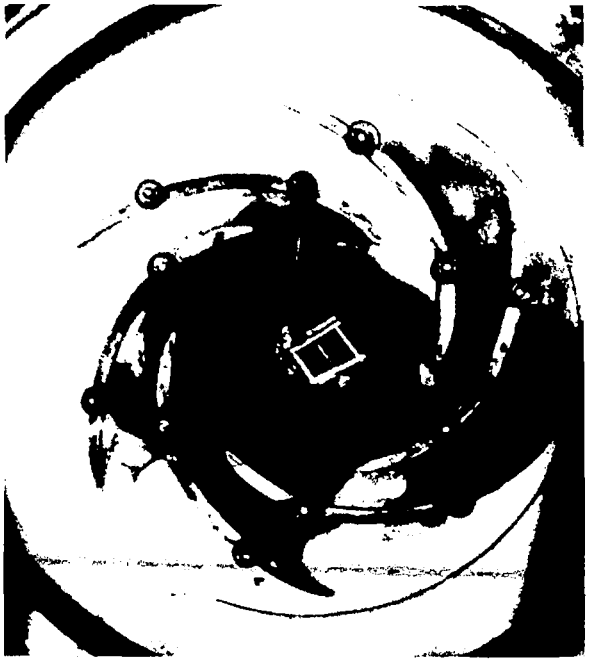

Figure 31.

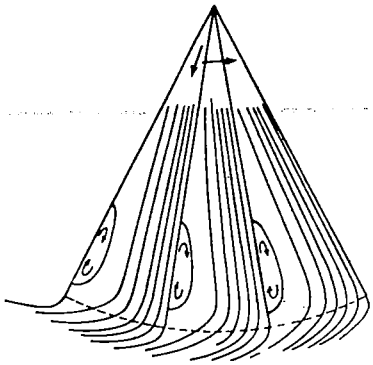

Figure 32.

Figure 33.

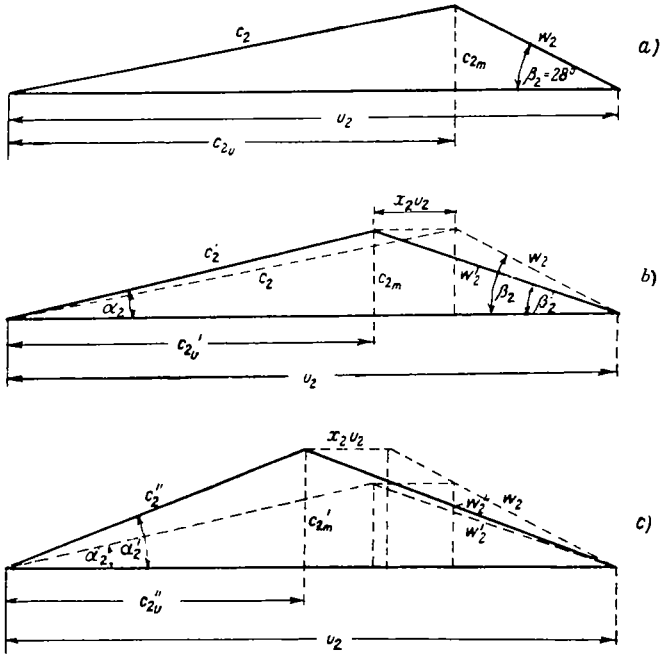

Figure 34.

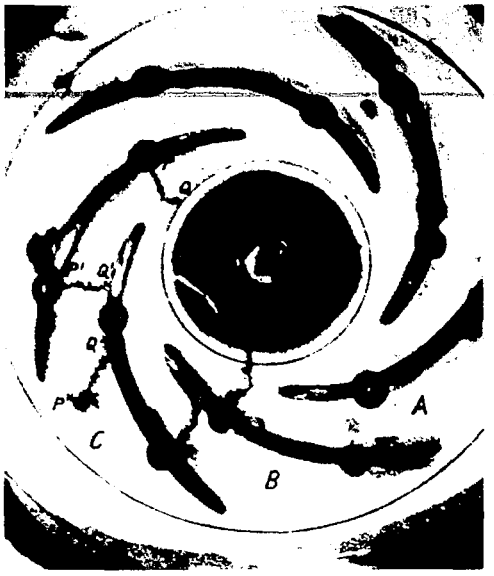

Figure 35.

Figure 36.

By
Author
Flow - Pumps, Centrifugal
Pumps, Centrifugal